

Research article

Characterization of subcellular localization and stability of a splice variant of G α_{i2}

Philip B Wedegaertner

Address: Department of Microbiology and Immunology Kimmel Cancer Institute Thomas Jefferson University 233 S. 10th St., 839 BLSB Philadelphia, PA 19107, USA

E-mail: P_Wedegaertner@mail.jci.tju.edu

Published: 31 May 2002

BMC Cell Biology 2002, 3:12

Received: 27 February 2002

Accepted: 31 May 2002

This article is available from: <http://www.biomedcentral.com/1471-2121/3/12>

© 2002 Wedegaertner; licensee BioMed Central Ltd. Verbatim copying and redistribution of this article are permitted in any medium for any purpose, provided this notice is preserved along with the article's original URL.

Abstract

Background: Alternative mRNA splicing of α_{i2} , a heterotrimeric G protein α subunit, has been shown to produce an additional protein, termed $s\alpha_{i2}$. In the $s\alpha_{i2}$ splice variant, 35 novel amino acids replace the normal C-terminal 24 amino acids of α_{i2} . Whereas α_{i2} is found predominantly at cellular plasma membranes, $s\alpha_{i2}$ has been localized to intracellular Golgi membranes, and the unique 35 amino acids of $s\alpha_{i2}$ have been suggested to constitute a specific targeting signal.

Results: This paper proposes and examines an alternative hypothesis: disruption of the normal C-terminus of α_{i2} produces an unstable protein that fails to localize to plasma membranes. $s\alpha_{i2}$ is poorly expressed upon transfection of cultured cells; however, radiolabeling indicated that α_{i2} and $s\alpha_{i2}$ undergo myristoylation, a co-translational modification, equally well suggesting that protein stability rather than translation is affected. Indeed, pulse-chase analysis indicates that $s\alpha_{i2}$ is more rapidly degraded compared to α_{i2} . Co-expression of $\beta\gamma$ rescues PM localization and increases expression of $s\alpha_{i2}$. In addition, $\alpha_{i2}A327S$, a mutant previously shown to be unstable and defective in guanine-nucleotide binding, and $\alpha_{i2}(1-331)$, in which the C-terminal 24 amino acids of α_{i2} are deleted, show a similar pattern of subcellular localization as $s\alpha_{i2}$ (i.e., intracellular membranes rather than plasma membranes). Finally, $s\alpha_{i2}$ displays a propensity to localize to potential aggresome-like structures.

Conclusions: Thus, instead of the novel C-terminus of $s\alpha_{i2}$ functioning as a specific Golgi targeting signal, the results presented here indicate that the disruption of the normal C-terminus of α_{i2} causes mislocalization and rapid degradation of $s\alpha_{i2}$.

Background

Heterotrimeric G proteins couple agonist-activated heptahelical receptors to a variety of effector responses. For the most part, this signaling activity takes place at the plasma membranes of cells. However, G proteins have been detected at a variety of subcellular locations and have been implicated in numerous membrane trafficking activities [1,2]. This suggests that distinct, though not yet deter-

mined, mechanisms exist to target G protein subunits to subcellular locations other than plasma membranes (PM). Furthermore, post-transcriptional or post-translational modifications may play a role in directing a G protein subunit to a specific intracellular location.

Unique subcellular localization has been observed for a novel alternative spliced form of the G protein α subunit

($G\alpha$), α_{i2} [3]. This α_{i2} splice variant, termed $s\alpha_{i2}$, contains a novel 35 amino acid sequence that replaces the C-terminal 24 amino acids of α_{i2} [3]. $s\alpha_{i2}$ has been observed to localize to Golgi membranes and other intracellular membranes [3,4]; in contrast, wild type α_{i2} is typically found at PM. Based on this unique localization of $s\alpha_{i2}$, a prominent role in membrane trafficking has been proposed for this subunit [3]. However, no report to date has supported a functional role for $s\alpha_{i2}$ in vesicular transport, although a variety of functional assays have implicated other $G\alpha$, including α_s and α_{i3} , in vesicle trafficking pathways [1,2].

In spite of its unknown functional significance, $s\alpha_{i2}$ provides a potential model for studying mechanisms of subcellular localization of $G\alpha$. Clearly, some aspect of the novel splicing is responsible for the difference in subcellular targeting of $s\alpha_{i2}$ (*i.e.*, Golgi and intracellular membranes) compared to wild type α_{i2} (*i.e.*, PM). To address the mechanism of subcellular localization of $s\alpha_{i2}$, two hypotheses were tested herein. First, the possibility was tested that the novel 35 amino acid sequence found at the C-terminus of $s\alpha_{i2}$ functions as a specific Golgi or intracellular membrane targeting motif. A second possibility was suggested by considering the location of the splice site. Several studies have shown that deletions or amino acid substitutions in the extreme C-terminal region of $G\alpha$ creates a protein defective in guanine-nucleotide binding [5–10]. Rapid release of guanine-nucleotides can result in an unstable $G\alpha$ [9,10]. This leads to the prediction that $s\alpha_{i2}$ is also unstable due to a disruption in the structure of its C-terminus caused by the novel splice sequence. Thus, the second possibility is that failure of $s\alpha_{i2}$ to localize at the PM but instead localize at intracellular membranes is the result of a general defect in protein stability. Results presented herein are consistent with this second hypothesis.

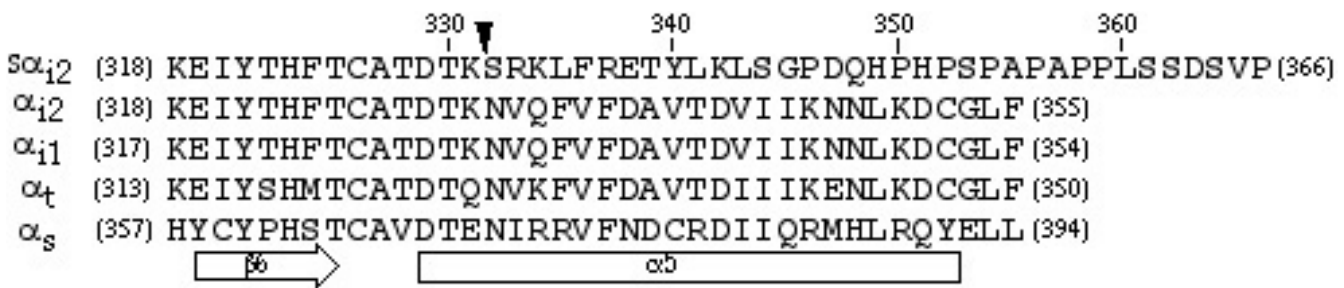
Results

α_{i2} and $s\alpha_{i2}$ differ only at their extreme C-termini. Alternative splicing results in a novel 35 amino acids in $s\alpha_{i2}$ that replace the C-terminal 24 amino acids of α_{i2} (Figure 1). In the studies presented here, both α_{i2} and $s\alpha_{i2}$ contain an internal EE epitope, as used previously for α_{i2} [11,12]. The use of the EE epitope allows the direct comparison of subcellular localization and expression of α_{i2} and $s\alpha_{i2}$, and facilitates immunoprecipitation of the two expressed proteins. This is essential since suitable antibodies to detect and immuno-isolate $s\alpha_{i2}$ are not readily available. Attempts to use a previously described polyclonal antibody directed against the C-terminus of $s\alpha_{i2}$ [3,4] were unsatisfactory in our hands. In particular, attempts to detect endogenous $s\alpha_{i2}$ by immunofluorescence failed due to faint detection that showed drastically different patterns of staining depending upon fixation technique.

The subcellular localization of expressed α_{i2} and $s\alpha_{i2}$ was compared in COS and BHK cells (Figure 2). In both cell types, α_{i2} was detected at cellular plasma membranes as highlighted by bright staining at the cell periphery (Figure 2A and 2C). In contrast, $s\alpha_{i2}$ was not detected at plasma membranes, but instead typically displayed an intracellular and perinuclear staining pattern (Figure 2B and 2D), consistent with localization to intracellular membranes as previously described [3,4]. The subcellular localization of $s\alpha_{i2}$ showed overlap in immunofluorescent staining with the Golgi protein, β -COP (Figure 3A and 3B) and the endoplasmic reticulum protein PDI (Figure 3C and 3D); localization of $s\alpha_{i2}$ exclusively to Golgi was not observed, even at the lowest levels of detection. Subcellular fractionation confirmed that $s\alpha_{i2}$ was localized, at least partly, to membranes (Figure 2E). After lysis of cells in hypotonic buffer followed by high-speed centrifugation, α_{i2} was found predominantly in the particulate fraction from COS (Figure 2E, lanes 3 and 4) or BHK cells (Figure 2E, lanes 9 and 10). A majority of $s\alpha_{i2}$ was also detected in the particulate fraction from both COS (Figure 2E, lanes 5 and 6) and BHK cells (Figure 2E, lanes 11 and 12), although some was also found in the soluble fraction. As a comparison, a non-palmitoylated mutant of α_q , in which cysteines 9 and 10 have been substituted with serines, is found predominantly in the soluble fraction (Figure 2E, lanes 7 and 8), as described previously [13]. Surprisingly, in comparison to α_{i2} , $s\alpha_{i2}$ was always detected in fewer cells, by immunofluorescence analysis, and showed lower levels of protein expression, by western blot analysis of subcellular fractions (Figure 2E) or whole cell lysates (not shown). These expression differences suggested that $s\alpha_{i2}$ was either less efficiently expressed or more rapidly degraded compared to α_{i2} , as described below.

The C-terminal 35 amino acids of $s\alpha_{i2}$, which replace the C-terminal 24 amino acids of α_{i2} (Figure 1), have been proposed to function as a Golgi targeting signal [3,4]. To test the potential importance of this C-terminal region in localization of $s\alpha_{i2}$ to intracellular membranes and prevention of $s\alpha_{i2}$ from localizing to PM, a deletion mutant of α_{i2} was constructed consisting of amino acids 1–331. In $s\alpha_{i2}$, the C-terminal splice occurs just after amino acid 331 (Figure 1), and thus the novel 35 amino acid splice sequence is removed in $\alpha_{i2}(1-331)$. Immunofluorescence microscopy indicates that $\alpha_{i2}(1-331)$ (Figure 4B) displays a subcellular localization pattern very similar to $s\alpha_{i2}$ (Figure 4A). This result is consistent with the alternative hypothesis that a disruption of α_{i2} at the C-terminus creates a protein unable to localize at the PM.

If the unique C-terminal 35 amino acid sequence of $s\alpha_{i2}$ functions as a Golgi targeting signal, it is important to test whether it is sufficient to target a heterologous protein to intracellular membranes. When the 35 amino acid se-

**Figure 1**

C-termini of G protein α subunits An alignment of C-terminal amino acids of selected G α is shown. The arrow indicates the site at which a novel 35 amino acids in α_{i2} replaces the C-terminal 24 amino acids of α_{i2} . Amino acid numbering is indicated in parentheses. Secondary structure is indicated at the bottom [19].

quence was fused to the C-terminus of GFP (GFP- α_{i2} 35aa), this unique α_{i2} sequence failed to direct GFP to intracellular membranes (Figure 5B); GFP- α_{i2} 35aa was diffusely distributed throughout the cytoplasm and nucleus, similar to what is observed for GFP alone (Figure 5A). On the other hand, when the first ten amino acids of α_{i2} are fused to GFP to create α_{i2} (1-10)-GFP, fluorescence is detected strongly at the PM (Figure 5C), indicating the N-terminus of α_{i2} , which contains the sites for myristoylation and palmitoylation [14], can be sufficient for directing PM localization of a normally cytosolic protein. In agreement with these results, the α_{i2} C-terminal sequence failed to redirect the localization of a secreted or a nuclear protein [4]. Thus, not only is the unique α_{i2} sequence unable to override other localization signals, it is unable to target a cytoplasmic protein to intracellular membranes. These results are consistent with a lack of a specific role for the α_{i2} sequence in Golgi membrane targeting.

The above experimental results failed to support the hypothesis that the unique 35 amino acid sequence from α_{i2} serves as a specific Golgi or intracellular membrane targeting motif. Thus, the following experiments concentrated on addressing the alternative hypothesis: α_{i2} is unstable and rapidly degraded due to disruptions in the C-terminus, and such instability results in a failure of α_{i2} to reach its proper place at the PM.

The ability of α_{i2} and α_{i2} to undergo N-terminal lipid modifications was compared. Myristoylation occurs co-translationally at the extreme N-terminal glycine, while palmitoylation occurs post-translationally at a cysteine immediately after the myristoylated glycine [15]. The subcellular site where palmitoylation occurs has not been well defined, although in one model palmitoylation occurs at the PM [16]. Cells expressing α_{i2} or α_{i2} were metabolically labeled with ^3H -palmitate or ^3H -myristate. α_{i2} and α_{i2} were immunoprecipitated from cell extracts, and

incorporation of radio-label was analyzed by SDS-PAGE followed by fluorography (Figure 6A). No palmitoylation of α_{i2} was detected (Figure 6A, lane 3), although α_{i2} was strongly palmitoylated (Figure 6A, lane 2). In contrast, both α_{i2} and α_{i2} incorporated similar levels of myristate (Figure 6A, lanes 5 and 6). The similar level of myristoylation was particularly surprising since total α_{i2} protein was much lower than α_{i2} as determined by immunoblotting of the immunoprecipitates (Figure 6B, compare lanes 5 and 6). Myristoylation is a co-translational modification, and levels of radio-labeling should thus reflect synthesis of new protein. Accordingly, the myristoylation results (Figure 6A and 6B, lanes 5 and 6) strongly suggested that α_{i2} and α_{i2} are translated equally well, as evidenced by similar levels of radiolabeled myristate incorporation during the labeling period, but α_{i2} is more rapidly degraded, as seen by reduced steady-state levels of immunoprecipitated protein. The lack of palmitoylation of α_{i2} is consistent with at least two, not necessarily mutually exclusive, possibilities. α_{i2} may fail to undergo palmitoylation because it is not stable long enough for post-translational palmitoylation to occur or because it fails to reach a PM site of palmitoylation. Alternatively, the novel C-terminal sequence of α_{i2} may somehow prevent direct recognition by a palmitoyl transferase.

Cells expressing high levels of α_{i2} , and to a much lesser extent α_{i2} , often displayed very bright intracellular accumulations of α_{i2} as visualized by immunofluorescence. These large spots were reminiscent of recently described aggresomes, accumulations of misfolded protein that are being targeted for proteasome-dependent degradation [17,18]. This observation suggested the possibility that intracellular localization of α_{i2} may reflect targeting to a proteasome-dependent degradative pathway. To test this idea further, cells expressing α_{i2} or α_{i2} were treated with the proteasome inhibitor acetyl-leucyl-leucyl-norleucinal (ALLN) and changes in localization of the α subunit were analyzed by immunofluorescence (Figure 7). After 1h

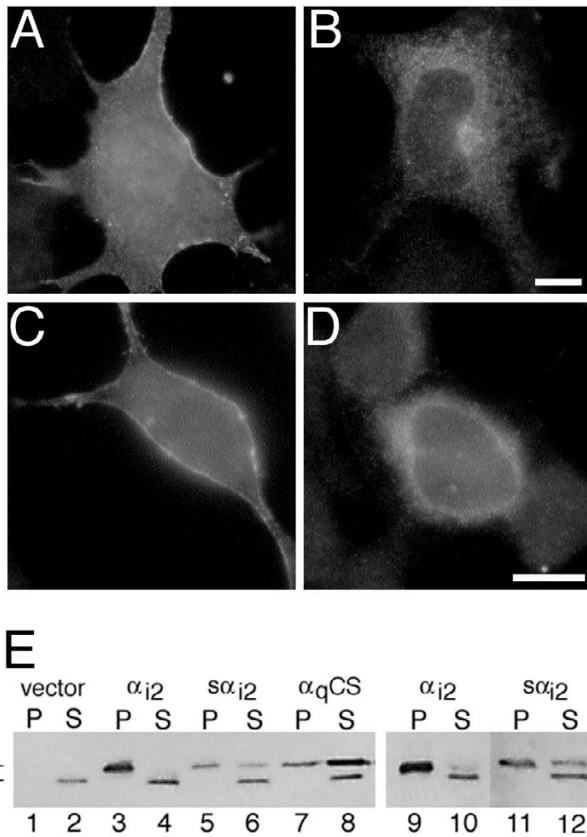


Figure 2
Localization of α_{i2} and $s\alpha_{i2}$ Expression vectors encoding α_{i2} (A and C) or $s\alpha_{i2}$ (B and D) were transiently transfected into COS-7 (A and B) or BHK (C and D) cells. Subcellular localization of the proteins was visualized by immunofluorescence microscopy using the EE monoclonal antibody followed by a Texas Red conjugated anti-mouse antibody, as described in "Materials and Methods". Bar, 10 μ m. E, pcDNA3 (lanes 1, 2), EE- α_{i2} -pcDNA3 (lanes 3, 4, 9, 10), EE- $s\alpha_{i2}$ -pcDNA3 (lanes 5, 6, 11, 12) or EE- α_qCS -pcDNA3 were transiently transfected into COS-7 (lanes 1-8) or BHK (lanes 9-12) cells. Cell lysates were separated into particulate (P) and soluble (S) fractions, as described in "Materials and Methods". EE-tagged G α subunits were detected at 41-45 kDa (double asterisk) by immunoblotting with the EE monoclonal antibody. A slightly smaller protein is consistently detected (denoted by single asterisk) by the EE antibody, and this background band fractionates exclusively to the soluble fraction.

treatment with ALLN, α_{i2} localization is relatively unaffected (Figure 7C), but $s\alpha_{i2}$ begins to show a slight increase in distinct intracellular accumulations (Figure 7D). At 4 h ALLN treatment, many cells expressing α_{i2} display a decrease in PM localization and an increase in intracellular staining (Figure 7E). α_{i2} is typically seen in large bright spots and in a perinuclear/intracellular membrane staining pattern after incubation of cells for 4 h with

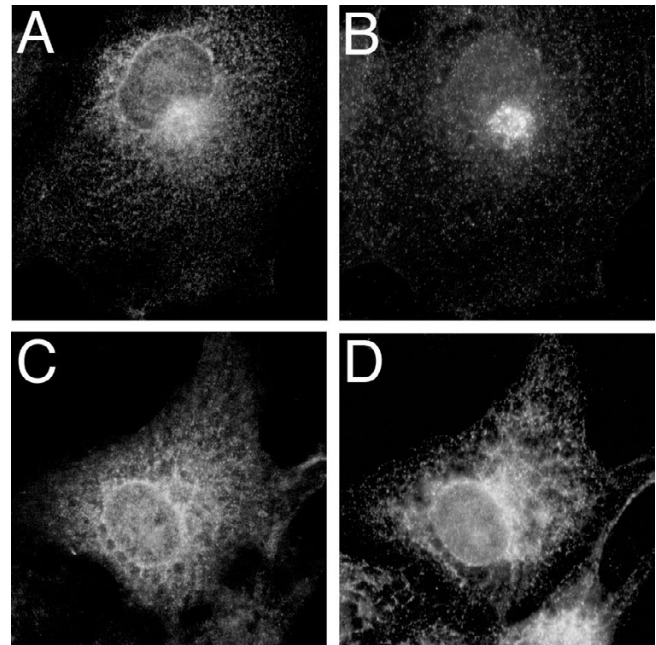


Figure 3
Localization of $s\alpha_{i2}$ to Golgi and ER membranes $s\alpha_{i2}$ was expressed in COS-7 cells. 48 h after transfection, cells on coverslips were fixed and processed for immunofluorescence. Co-localization of $s\alpha_{i2}$ (A) and the Golgi protein, β -COP (B), was visualized after incubation of cells with the EE antibody and a rabbit polyclonal anti- β -COP antibody followed by Alexa 594 anti-mouse and Alexa 488 anti-rabbit antibodies. Co-localization of $s\alpha_{i2}$ (C) and the endoplasmic reticulum protein, protein disulfide isomerase (PDI) (D), was visualized after incubation of cells with the EE antibody and a rabbit polyclonal anti-PDI antibody followed by Alexa 594 anti-mouse and Alexa 488 anti-rabbit antibodies.

ALLN. In fact, the localization pattern of α_{i2} after 4 h incubation with ALLN (Figure 7E) is similar to the observed localization of $s\alpha_{i2}$ in the absence or presence of ALLN treatment (Figure 7B, 7D, and 7F). At 8 h treatment with ALLN, both α_{i2} (Figure 7G) and $s\alpha_{i2}$ (Figure 7H) are detected almost exclusively as a large bright spot in each expressing cell. Similar results were obtained using another proteasome inhibitor, MG-132. Interestingly, ALLN treatment was relatively ineffective at promoting accumulation of overexpressed α_s in aggresome-like structures (not shown). Thus, the results of Figure 7 are consistent with the proposal that the intracellular localization of $s\alpha_{i2}$ is due to its targeting to a degradative pathway, a pathway shared by α_{i2} .

The subcellular localization of $s\alpha_{i2}$ was compared to $\alpha_{i2}A327S$. This alanine to serine mutation in the C-terminal region of α_{i1} (A326S) and α_s (A366S) has been shown to greatly accelerate GDP release, to accelerate irreversible inactivation *in vitro*, and to cause rapid turnover of the α

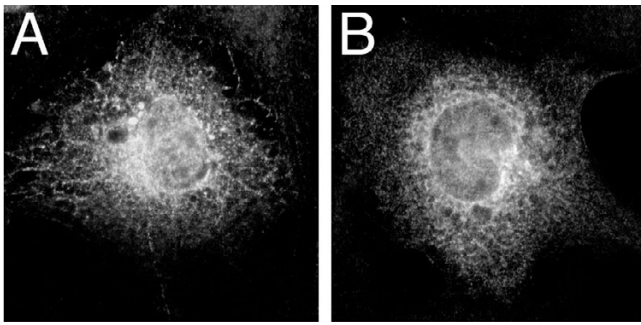


Figure 4
Localization of $s\alpha_{i2}$ and $\alpha_{i2}(1-331)$ Expression vectors encoding $s\alpha_{i2}$ (A) or $\alpha_{i2}(1-331)$ (B) were transiently transfected into COS-7 cells. 48 h after transfection, subcellular localization of the proteins was visualized by immunofluorescence microscopy using the EE monoclonal antibody followed by Alexa 594 anti-mouse antibody, as described in "Materials and Methods".

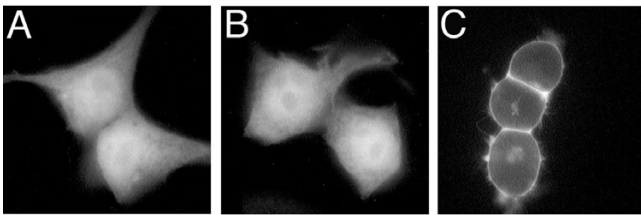


Figure 5
C-terminal 35 amino acids of $s\alpha_{i2}$ do not affect GFP localization Expression vectors encoding GFP (A), GFP- $s\alpha_{i2}35aa$ (B), or $\alpha_{i2}(1-10)$ -GFP (C) were transfected into HEK293 cells. 48 h after transfection, cells were fixed on coverslips, and subcellular localization was determined by fluorescence microscopy visualization of GFP.

subunit in cultured cells [9,10]. Thus, if the observed intracellular localization of $s\alpha_{i2}$ is caused by instability of the protein due to disruptions at its C-terminus, then it follows that $\alpha_{i2}A327S$ should show a similar pattern of localization. Indeed, immunofluorescence microscopy revealed a pronounced intracellular distribution for $\alpha_{i2}A327S$ (Figure 8E). In addition to intracellular membrane localization similar to $s\alpha_{i2}$ (Figure 8C), $\alpha_{i2}A327S$ was detected weakly but consistently at the PM. It seems likely that the C-terminal disruption of $s\alpha_{i2}$ (replacing the 24 C-terminal amino acids) is a more severe disruption than the A327S substitution. Thus, the similarity in localization of $s\alpha_{i2}$ and $\alpha_{i2}A327S$ bolsters the idea that mislocalization of $s\alpha_{i2}$ is caused by its inherent instability.

G protein $\beta\gamma$ subunits can stabilize wild type and alanine to serine mutant α subunits *in vitro* [10]. Thus, the effect of $\beta\gamma$ co-expression on subcellular localization of $\alpha_{i2}A327S$ and $s\alpha_{i2}$ was tested. α_{i2} localizes to the PM efficiently

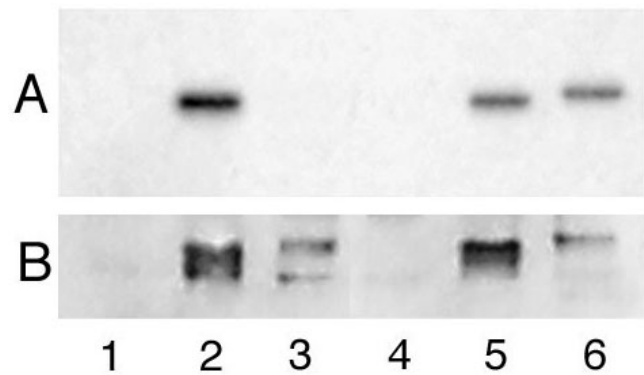


Figure 6
Myristoylation and palmitoylation of α_{i2} and $s\alpha_{i2}$ COS-7 cells were transfected with pcDNA3 (lanes 1 and 4), or pcDNA3 containing α_{i2} (lanes 2 and 5) or $s\alpha_{i2}$ (lanes 3 and 6). 48 h after transfection, cells were incubated with 1.0 mCi/ml 3H -palmitate (lanes 1-3) or 0.5 mCi/ml 3H -myristate (lanes 4-6) for 2 h. Following immunoprecipitation with the EE antibody, duplicate samples were resolved by SDS-PAGE. Radiolabeled proteins were visualized by fluorography (panel A), and immunoblotting with the EE antibody provides a comparison of protein levels of α_{i2} and $s\alpha_{i2}$ (panel B).

when expressed alone (Figure 8A) or when co-expressed with $\beta\gamma$ (Figure 8B). $s\alpha_{i2}$ shows a dramatic change in localization when co-expressed with $\beta\gamma$ (Figure 8D), displaying strong PM staining. Not only is $s\alpha_{i2}$ targeted efficiently to the PM when co-expressed with $\beta\gamma$, but $\beta\gamma$ co-expression increases overall levels of transiently expressed $s\alpha_{i2}$ and α_{i2} , as determined by immunoblotting (Figure 8G), and increases the number of cells expressing $s\alpha_{i2}$, as observed by immunofluorescence microscopy (not shown). Similarly, co-expression of $\beta\gamma$ efficiently promotes PM localization of $\alpha_{i2}A327S$ (Figure 8F).

The analysis of the effect of $\beta\gamma$ was extended by examining the localization of α_{i2} or $s\alpha_{i2}$ after co-transfection with $\beta\gamma$ and after treatment with ALLN. In contrast to Figure 7, a marked difference was observed between α_{i2} and $s\alpha_{i2}$ after ALLN treatment. When $\beta\gamma$ is co-expressed with α_{i2} , PM localization of α_{i2} is observed, as shown in Figure 8B, and incubation with ALLN for 8 h shows little effect on PM localization of α_{i2} (Figure 9A). When $\beta\gamma$ is co-expressed with $s\alpha_{i2}$, PM localization of $s\alpha_{i2}$ is observed, as shown in Figure 8D, but incubation with ALLN for 8 h causes an increase in bright intracellular accumulations of $s\alpha_{i2}$ (Figure 9B). Taken together, results with $\beta\gamma$ co-expression are consistent with the ability of $\beta\gamma$ to promote PM targeting of $G\alpha$, and further suggest that $s\alpha_{i2}$ is less effectively stabilized than α_{i2} by $\beta\gamma$, as evidenced by ALLN-induced accumulation in intracellular aggregates (Figure 9B).

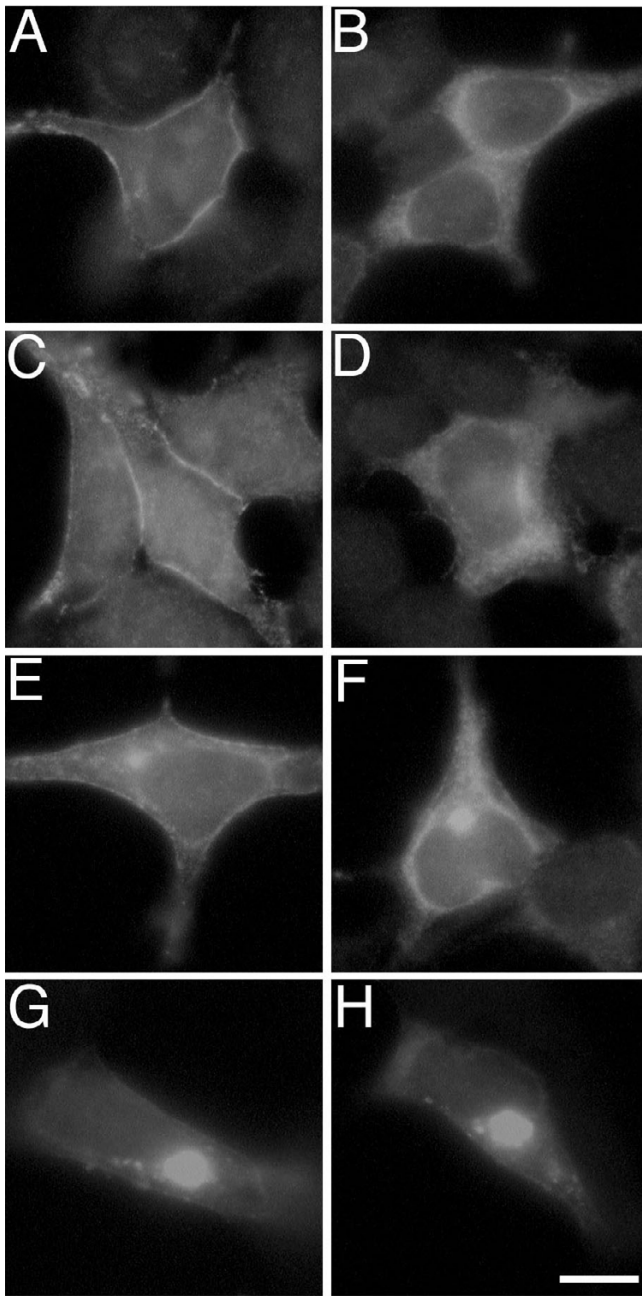


Figure 7
Effect of ALLN on α_{i2} and $s\alpha_{i2}$ localization α_{i2} (A, C, E, and G) or $s\alpha_{i2}$ (B, D, F, and H) was expressed in BHK cells. 48 h after transfections cells were incubated in the absence (A and B) or presence of 20 $\mu\text{g/ml}$ ALLN for 1 h (C and D), 4 h (E and F), or 8 h (G and H). Cells were fixed and processed for immunofluorescence using the EE antibody followed by an Alexa 488 conjugate anti-mouse antibody. Bar, 10 μm .

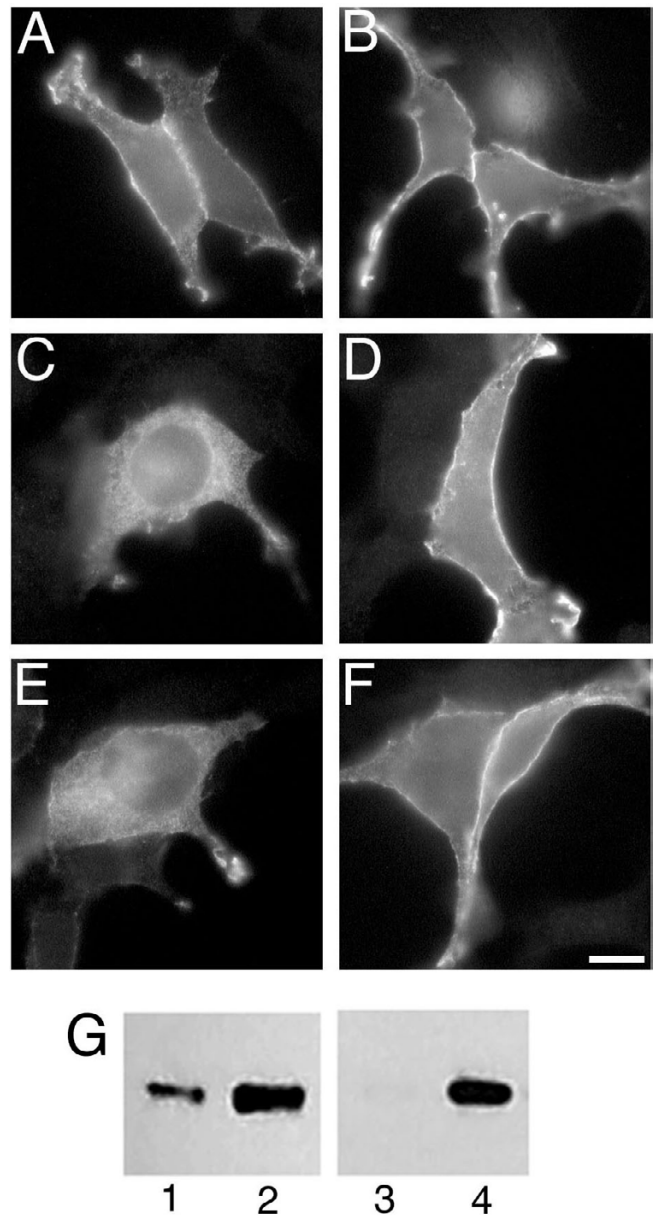


Figure 8
Localization of α_{i2} , $s\alpha_{i2}$, and $\alpha_{i2}\text{A327S}$ and the effect of $\beta\gamma$ Expression vectors encoding α_{i2} (A and B), $s\alpha_{i2}$ (C and D), or $\alpha_{i2}\text{A327}$ (E and F) were transfected alone (A, C, and E) or together with expression vectors for β_1 and γ_2 (B, D, and F) into BHK cells. Proteins were visualized by immunofluorescence microscopy using the EE monoclonal antibody followed by an Alexa 488 conjugate anti-mouse antibody. Bar, 10 μm . G, EE- α_{i2} -pcDNA3 (lanes 1 and 2) or EE- $s\alpha_{i2}$ -pcDNA3 (lanes 3 and 4) were transfected into COS-7 cells alone (lanes 1 and 3) or with co-transfection of vectors encoding β_1 and γ_2 (lanes 2 and 4). Immunoblotting with the EE antibody detected α_{i2} or $s\alpha_{i2}$. Note that $s\alpha_{i2}$ expressed alone (lane 3) is very weakly detected and barely visible in this total cell lysate.

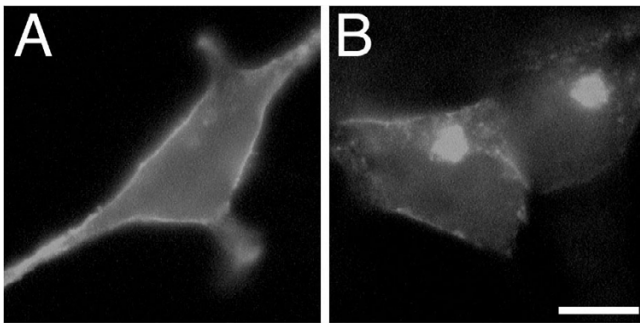


Figure 9
Effect of ALLN on α_{i2} and $s\alpha_{i2}$ localization when co-expressed with $\beta\gamma$ Expression vectors encoding α_{i2} (A) or $s\alpha_{i2}$ (B) were transfected together with expression vectors for β_1 and γ_2 into BHK cells. 48 h after transfections cells were incubated in the presence of 20 $\mu\text{g/ml}$ ALLN for 8 h. Cells were fixed and processed for immunofluorescence using the EE antibody followed by an Alexa 594 conjugate anti-mouse antibody. Bar, 10 μm .

Lastly, ^{35}S -methionine pulse-chase labeling studies directly confirmed that $s\alpha_{i2}$ was more rapidly degraded than α_{i2} (Figure 10). After transient expression of the α subunits, cellular proteins were radiolabeled with a brief pulse of ^{35}S -methionine followed by a chase. Immunoprecipitation of the α subunit after increasing times of chase, followed by SDS-PAGE and fluorography revealed that radiolabeled $s\alpha_{i2}$ was rapidly lost. α_{i2} consistently displayed a 3–4 fold longer half-life compared to $s\alpha_{i2}$, while $\alpha_{i2}\text{A327S}$ was intermediate. In the experiment presented in Figure 10, the $t_{1/2}$ was determined to be approximately 90, 180, and 360 min for $s\alpha_{i2}$, $\alpha_{i2}\text{A327S}$, and α_{i2} , respectively. Although this trend was consistent, the exact $t_{1/2}$ showed some variability from experiment to experiment, probably due to varying levels of transient overexpression. It is likely that the difference in turnover of $s\alpha_{i2}$ and α_{i2} is even more profound when the proteins are expressed at lower levels. Consistent with this idea, $s\alpha_{i2}$ was refractory to stable expression even though cells stably expressing α_{i2} were easily selected (not shown). The inability to isolate cells stably expressing $s\alpha_{i2}$ can be attributed to its rapid degradation. Regardless, ^{35}S -methionine pulse-chase labeling studies (Figure 10) demonstrate that $s\alpha_{i2}$ is indeed more rapidly degraded than α_{i2} .

Discussion

In addition to their well characterized role at the PM in coupling activated GPCRs to effector proteins, heterotrimeric G proteins have been implicated in a variety of other cellular functions, including membrane trafficking pathways. A splice variant of α_{i2} , termed $s\alpha_{i2}$, has been proposed as a candidate to regulate vesicle transport due to its localization at intracellular membranes. The studies described in this report were undertaken to define mech-

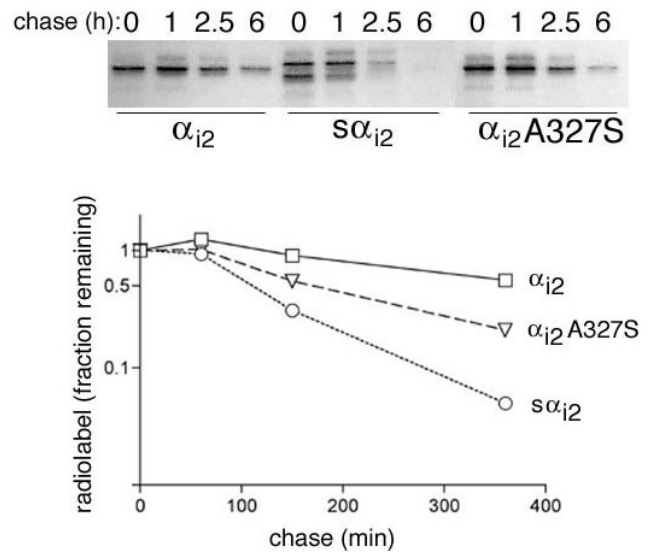


Figure 10
Pulse-chase analysis of α_{i2} , $s\alpha_{i2}$, and $\alpha_{i2}\text{A327S}$ Expression vectors encoding α_{i2} , $s\alpha_{i2}$, or $\alpha_{i2}\text{A327S}$ were transfected into COS-7 cells. 48 h after transfection, cells were incubated for 10 min in media containing 0.1 mCi/ml ^{35}S Express protein labeling mix. Cells were washed, and incubated in regular media for the indicated times (chase). Cells were harvested, lysates were prepared, and immunoprecipitations were performed using the EE antibody. Samples were resolved by SDS-PAGE, and radiolabeled proteins were visualized by fluorography (upper panel). Note that two bands are present in the $s\alpha_{i2}$ lanes; the upper band represents full-length $s\alpha_{i2}$ and quantitation of this band was used to determine a half-life. The lower band likely represents a degradation product of $s\alpha_{i2}$ that is itself degraded even faster. Quantitation of the bands from the fluorograph was performed by densitometry and plotted as degradation curves (lower panel) for α_{i2} (\square), $s\alpha_{i2}$ (\circ), and $\alpha_{i2}\text{A327S}$ (∇). These experiments were repeated and the average \pm S.E. half-life was determined as 237 ± 110 , 150 ± 42 , and 67 ± 21 min for α_{i2} ($n = 3$), $\alpha_{i2}\text{A327S}$ ($n = 2$), and $s\alpha_{i2}$ ($n = 3$), respectively.

anisms that underlie subcellular localization of $s\alpha_{i2}$. The novel 35 amino acids found in $s\alpha_{i2}$ appear not to function as a specific Golgi or endoplasmic reticulum targeting sequence. Instead, the results in this study support the proposal that $s\alpha_{i2}$ fails to target to the PM because it is an unstable protein. The following results support this hypothesis: 1) $s\alpha_{i2}$ and α_{i2} are equally labeled by a pulse of ^3H -myristate, although much less $s\alpha_{i2}$ protein is detected; 2) $s\alpha_{i2}$ displays a propensity to localize to potential aggregate-like structures, and this localization is greatly enhanced by proteasome inhibitor treatment; 3) the $\alpha_{i2}\text{A327S}$ mutant, previously shown to be unstable and defective in guanine-nucleotide binding, shows a similar pattern of subcellular localization (*i.e.*, intracellular membranes rather than PM); 4) $\beta\gamma$ over-expression increases

expression of α_{i2} and promotes PM localization of α_{i2} and $\alpha_{i2}A327S$, but $\beta\gamma$ co-expression does not prevent α_{i2} localization to potential aggresome-like structures when cells are treated with proteasome inhibitors; and 5) pulse-chase analysis indicates that α_{i2} is rapidly degraded.

A number of reports have demonstrated that disruptions in the C-termini of $G\alpha$ cause reduced affinity for guanine-nucleotides and protein instability. The C-terminal 30 amino acids of $G\alpha$ consist of the $\beta 6$ - $\alpha 5$ loop, followed by the $\alpha 5$ helix and finally several amino acids of flexible structure (Figure 1) [19–21]. The $\beta 6$ - $\alpha 5$ loop stabilizes the guanine ring of bound GDP or GTP, and mutations in this region affect guanine-nucleotide binding. The A326S mutation of α_{i1} and A366S mutation of α_s (cognate to the $\alpha_{i2}A327S$ used in this study) were shown to cause greatly decreased affinity for GDP [9,10]. Defective binding of GDP leads to more $G\alpha$ in the empty state (no bound guanine-nucleotide), and this form of $G\alpha$ is rapidly denatured *in vitro*, as shown for α_sA366S and $\alpha_{i1}A326S$ [9,10]. Moreover, α_sA366S was demonstrated to undergo rapid degradation ($t_{1/2} < 1$ h) in stably transfected cells [9]. The same mutation in α_t has also been shown to greatly decrease guanine-nucleotide binding [5,22]. Additional amino acids in the critical $\beta 6$ - $\alpha 5$ loop are important for maintaining $G\alpha$ integrity [7].

Although the $\alpha 5$ helix (Figure 1) does not directly contact the bound guanine-nucleotide [19–21], it is clearly important for $G\alpha$ structure and to maintain the proper orientation of the $\beta 6$ - $\alpha 5$ loop. A recent study identified a number of $\alpha 5$ helix residues in α_t that when changed to alanines increased rates of guanine-nucleotide exchange (*i.e.*, decreased affinity for guanine-nucleotides) [5]. Individual mutation of amino acids in α_v , cognate to T330, N332, V333, F337 in α_{i2} (Figure 1), increased nucleotide exchange rates [5]. Two of these critical amino acids, N332 and V333 in α_{i2} , are in fact the first two amino acids that are replaced by the novel splicing in α_{i2} (Figure 1). Thus, one might speculate that the novel 35 amino acid sequence in α_{i2} would impair guanine-nucleotide binding and result in an unstable protein. Unfortunately, initial attempts to directly show a defect in guanine-nucleotide binding by α_{i2} , using a GTP γ S-dependent trypsin protection assay [23], were unsuccessful due, at least in part, to the inability to solubilize expressed α_{i2} from membranes using a mild detergent (*e.g.*, lubrol/polyoxyethylene 10-lauryl ether).

The data in this report are consistent with a scenario in which intracellular Golgi/ER localization of α_{i2} reflects its rapid degradation rather than specific targeting to a subcellular organelle. Particularly compelling is the similarity in subcellular localization of $\alpha_{i2}A327S$ and α_{i2} (Figure 8). In addition, the use of proteasome inhibitors

(Figures 7 and 9) suggest that α_{i2} is degraded by a proteasome pathway. The observed intracellular membrane (ER) localization and proteasome inhibitor-induced juxtannuclear aggregate accumulation (aggresome) is consistent with that reported for other proteins being degraded by such a pathway [18,24]. When treated with proteasome inhibitors, overexpressed wild type α_{i2} also accumulates in aggresome-like structures (Figure 7), suggesting that $G\alpha$ may normally be degraded by a proteasome-dependent pathway. However, over-expression of $\beta\gamma$ prevents ALLN-induced juxtannuclear accumulations of α_{i2} but not α_{i2} (Figure 9). Although little is known regarding degradative pathways for G proteins, α_{i2} and other mutants (*e.g.*, $\alpha_{i2}A327S$) may be valuable tools for defining such pathways.

The data presented here argue against a sequence specific Golgi membrane targeting function for the novel 35 amino acid sequence found in α_{i2} . The novel sequence of α_{i2} is not sufficient to direct other proteins to Golgi/ER membranes. These 35 amino acids did not change the cytoplasmic localization of GFP (Figure 5). Similarly, a recent report showed that the α_{i2} 35 amino acids were unable to retain a secreted protein in intracellular membranes and did not affect localization of a nuclear protein [4]. However, in addition to causing rapid degradation, one cannot rule out that the 35 amino acid sequence of α_{i2} functions somehow as part of a Golgi targeting motif in the context of other regions of α_{i2} , as suggested [4]. Other researchers have described a specific Golgi membrane localization of α_{i2} [4]; in contrast, the results presented in this report always show a much more diffuse subcellular localization of α_{i2} to intracellular membranes consistent with staining of both Golgi and ER. The reason for this difference in localization is unclear. Interestingly, in the other study, the authors found that deletion of a proline-rich sequence corresponding to α_{i2} amino acids 348–359 (Figure 1) changed localization of α_{i2} from Golgi membranes to a more diffuse localization throughout intracellular membranes [4]. However, mutation of proline residues to alanines failed to affect α_{i2} localization [4]. Thus, little evidence exists to support a specific membrane targeting role for the novel α_{i2} sequence.

$\beta\gamma$ was able to promote plasma membrane localization of α_{i2} (Figure 8). $\beta\gamma$ prevents irreversible inactivation of α_{i1} , when measured *in vitro* at 37°C, and slows the inactivation of $\alpha_{i1}A326S$ [10]. Thus, $\beta\gamma$ may stabilize α_{i2} and $\alpha_{i2}A327S$ allowing $\beta\gamma$ -dependent [25–29] PM localization. These results are also consistent with the possibility that the primary defect in α_{i2} is a reduced ability to interact with $\beta\gamma$; $G\alpha$ containing mutations in known sites of contact with $\beta\gamma$ fail to localize to PM, but over-expression of $\beta\gamma$ can rescue their PM localization [28,29]. However,

the crystal structures [30,31] show that the C-terminal $\beta 6$ - $\alpha 5$ loop/ $\alpha 5$ helix region does not directly contact $\beta \gamma$. Thus, it is more likely that indeed α_{i2} is deficient in binding to $\beta \gamma$, but this effect is a consequence of its instability. α_{i2} may exist in a state that does not interact well with $\beta \gamma$ simply because it is in the process of being irreversibly inactivated [9,10]. Similarly, $\alpha_{i2}A327S$ appears not to be defective in its intrinsic ability to interact $\beta \gamma$ [10], and co-expression of $\beta \gamma$ shifts $\alpha_{i2}A327S$, like α_{i2} , from intracellular to plasma membranes (Figure 8).

What is the cellular function of α_{i2} ? The ability of $\beta \gamma$ to promote PM localization of α_{i2} raises the possibility that endogenous α_{i2} is in fact localized to PM where it can interact with GPCRs and effectors. Future studies will test the potential of α_{i2} , when co-expressed with $\beta \gamma$, to productively interact with receptors and effectors. However, this possibility is viewed as unlikely for several reasons. First, others have shown that in COS-7 cells endogenous α_{i2} is not detected at PM but only found intracellularly [3,4], although one cannot rule out that a small but functionally significant fraction of α_{i2} reaches the PM. Second, the extreme C-termini of $G\alpha$ are critical sites for interaction with GPCRs [32], and the novel C-terminal sequence found in α_{i2} would be predicted to disrupt productive interactions with GPCRs. Third, even though $\beta \gamma$ can promote PM localization of α_{i2} in the overexpression system described here, α_{i2} remains less stable than α_{i2} (Figure 9), suggesting that such instability may also impair productive interactions with GPCRs.

On the other hand, unknown protein(s) may function to stabilize α_{i2} and help direct it to Golgi membranes. A specific combination of β and γ subtypes may play such a role; however, one thorough study showed a lack of $\beta \gamma$ on Golgi membranes of exocrine pancreatic cells even though a variety of $G\alpha$ were readily detected in the Golgi [33]. Other proteins that may specifically promote the intracellular targeting of $G\alpha$ have not been identified.

It is possible that α_{i2} functions as a short-lived protein regulating some aspect of membrane transport pathways; however, no experiments to directly support or refute this hypothesis have been reported. Instead, it is tempting to speculate that alternative splicing may be a mechanism to regulate cellular levels of α_{i2} . In this model, certain conditions may favor the formation of α_{i2} compared to α_{i2} , and the resulting rapid degradation of α_{i2} would decrease the cellular content of α_{i2} . A precedent for such alternative splicing-dependent regulation of expression has been described for H-ras [34]. Alternative splicing occurs in H-ras, and the alternative spliced form is predicted to encode an unstable transcript and a protein product that lacks the ability to oncogenically transform cells. A mutation was identified that abolishes the alternatively spliced

form, and this mutation leads to an increase in H-ras expression and transforming ability. Thus, it was demonstrated that alternative splicing is a mechanism that cells use to control expression of H-ras [34]. Alternative splicing may similarly play an important role in regulating expression of α_{i2} . Testing of this idea will require a comparison of α_{i2} and α_{i2} transcript levels, and an analysis of whether relative expression is affected in response to physiological changes, such as extracellular stimuli or cell differentiation.

Conclusions

In summary, the results presented here demonstrate that α_{i2} , a novel splice variant of α_{i2} , is rapidly degraded when expressed in cells. Such instability is consistent with known structure-function data regarding the importance of the C-terminus of $G\alpha$ subunits. The observed intracellular localization of α_{i2} is due, at least in part, to its instability. Moreover, the data presented in this study argue against the novel C-terminus of α_{i2} functioning as a specific Golgi targeting motif.

In addition, similarly to α_{i2} , an α_{i2} mutant, $\alpha_{i2}A327S$, previously demonstrated to be unstable *in vitro*, displays a defect in plasma membrane localization when expressed in cells. These results suggest that both α_{i2} and $\alpha_{i2}A327S$ may prove valuable in future studies of mechanisms of degradation of $G\alpha$.

Materials and methods

Materials

Cell culture reagents were obtained from Mediatech. [9,10-³H]palmitic acid, [9,10-³H]myristic acid, and ³⁵S Express labeling mix were from NEN. Acetyl-leucyl-leucyl-norleucinal (ALLN) and MG-132 were from Calbiochem. The EE monoclonal antibody was a gift from H. Bourne. Other reagents were obtained from Fisher and Sigma.

Expression plasmids

EE- α_{i2} -pcDNA1 was obtained from H. Bourne (UCSF). In this plasmid, mouse α_{i2} cDNA contains the EE epitope sequence EEYMPTE at codons 166 to 172 [11]. Mouse α_{i2} cDNA was provided by E. Borrelli (Strasbourg) in the plasmid pSVsGi2. α_{i2} was excised from pSVsGi2 using EcoRI and SmaI and subcloned into the EcoRI and EcoRV sites of pcDNA1 to produce α_{i2} -pcDNA1. EE-tagged α_{i2} was constructed by subcloning a EcoRI-BglII fragment from EE- α_{i2} -pcDNA1 into α_{i2} -pcDNA1. EE-tagged $\alpha_{i2}A327S$ -pcDNA1 was obtained from J. Morales (UCSF). EE-tagged $\alpha_{i2}(1-331)$ -pcDNA3 was constructed by PCR amplification of the coding region for the amino acids 1 to 331 of α_{i2} using the T7 primer as the 5' primer and 5'-ccggctcgagtcactgtcgggtcggggcgcgatg-3' as the 3' primer and using EE- α_{i2} -pcDNA3 as the template. The PCR amplified product was digested with HindIII and XhoI and subcloned

into the correspondingly digested EE- α_{i2} -pcDNA3. GFP- α_{i2} 35aa was constructed by PCR amplification of the coding region for the C-terminal 35 amino acids of α_{i2} using the 5' primer 5'-cgcatctagaaaactttttaga-3' and the 3' primer 5'-cgcaagcttactcaaggcacggaatc-3'. The PCR fragment was digested with BglII and HindIII and subcloned into the correspondingly digested pEGFP-C1 (Clontech). α_{i2} (1-10)-GFP was constructed by annealing the complementary oligonucleotides 5'-ctagcaccatgggctgcaccgtgctg-cgcaggacaag-3' and 5'-ccggcttgcctcggacacgggtgcagccatggtg-3' (corresponding to amino acids 1-10 of α_{i2}) and ligating into AgeI-NheI digested pEGFP-N1. Human β_1 -pCMV5 and bovine γ_2 -pcDNAI have been described [35].

Cell culture and transfection

BHK, HEK293, and COS-7 cells were cultured in DMEM containing 10% fetal bovine serum. Transfections were performed in 6-well plates or 6 cm culture dishes using Lipofectamine (GibcoBRL) or FuGene6 (Roche) according to the manufacturer's protocol.

Immunofluorescence localization

Cells were transfected in 6-well plates with 1 μ g of the indicated expression plasmid. In experiments where β_1 and γ_2 expression plasmids were co-transfected with α_{i2} or α_{i2} , the amounts of α , β , and γ plasmids used were 0.7, 0.2, and 0.1 μ g, respectively. 24 h after transfection, cells were replated onto glass coverslips and grown for an additional 24 h before fixing in methanol at -20°C for 20 min. Cells were washed with PBS and then incubated in blocking buffer consisting of TBS (50 mM Tris, pH 7.5, 150 mM NaCl) with 1% Triton X-100 and 2.5% nonfat milk. Coverslips were then incubated in blocking buffer containing 20 μ g/ml EE monoclonal antibody for 1 h. For dual localization experiments, a 1:1000 dilution of a rabbit polyclonal anti- β -coatamer protein (β -COP) antibody (Affinity BioReagents) or a 1:200 dilution of a rabbit polyclonal anti-protein disulfide isomerase (PDI) antibody (Stress-Gen Biotechnologies) was included with the EE mouse monoclonal. Following washes with blocking buffer, cells were incubated in a 1:100 dilution of the indicated secondary antibody, either Alexa Fluor 488 or 594 goat anti-mouse (Molecular Probes) or Texas Red donkey anti-mouse (Jackson ImmunoResearch) or Alexa Fluor 488 goat anti-rabbit (Molecular Probes), for 30 min. The coverslips were washed and mounted on glass slides with Prolong Antifade reagent (Molecular Probes, Eugene, OR), and microscopy was performed with an Olympus BX60 microscope equipped with a Sony DKC-5000 digital camera. A minimum of 50 cells were examined for each transfection. Transfections were repeated and representative pictures were taken of cells displaying a typical expression pattern for each transfection. Only cells displaying

low to intermediate levels of expression were utilized. Images were processed with Adobe Photoshop.

Subcellular Fractionation

Soluble and particulate fractions were isolated as previously described [29]. BHK or COS-7 cells were transfected in 6 cm plates with 3 μ g of the indicated expression plasmid. 24 h after transfection, the cells were transferred to 10-cm plates and grown for another 24 h. Cells were washed with phosphate-buffered saline and then lysed in 0.5 ml hypotonic lysis buffer by 10 passages through a 27-gauge needle. Cells were centrifuged at 200 \times g for 5 min to pellet nuclei and intact cells, and the supernatant was then centrifuged at 150,000 \times g for 20 min to obtain soluble and particulate fractions. Fractions were resolved by 12% SDS-PAGE, transferred onto PVDF-Plus (Micron Separations, Inc) and probed with EE monoclonal antibody. Bands were visualized by chemiluminescence.

Metabolic labeling and immunoprecipitation

COS-7 cells were transfected in 6 cm plates with 3 μ g of the indicated expression plasmid. 24 h after transfection, cells were replated into 6 cm plates. For fatty acid labeling experiments [36], one transfection was replated into two 6 cm plates. For 35 S labeling experiments, cells from two or three identical transfections were combined before replating in multiple 6 cm plates. Incubation with radioisotope was then performed 48 h after transfection.

For fatty acid labeling, cells in a 6 cm dish were incubated with 1 ml of DMEM containing 10% dialyzed fetal bovine serum, 5 mM sodium pyruvate, and [9,10- 3 H]palmitic acid (1 mCi/ml) or [9,10- 3 H]myristate (0.5 mCi/ml) for 2 h. For 35 S pulse-chase labeling, cells in a 6 cm dish were washed with DMEM (without methionine), and then incubated in DMEM (without methionine) containing 10% dialyzed fetal bovine serum at 37°C for 1 h. Next, cells were incubated in DMEM (without methionine) containing 10% dialyzed fetal bovine serum and 0.1 mCi/ml 35 S Express mix for 10 min. After the 10 min pulse labeling, cells were either immediately lysed (see below) or washed with normal growth media and then "chased" by incubation in normal growth media for the indicated times.

Fatty acid labeled and 35 S methionine/cysteine labeled samples were then identically processed by immunoprecipitation. Cells were washed once with ice-cold PBS and lysed in 1 ml of Extraction buffer (50 mM HEPES, pH 8, 50 mM NaCl, 10 μ M β -mercaptoethanol, 1% Triton X-100, 1% sodium cholate, 1 mM PMSF, 2 μ g/ml leupeptin, and 2 μ g/ml aprotinin). Cell extracts were tumbled for 1 h at 4°C, and nuclei and insoluble material were removed by microcentrifugation at 16,000 \times g for 3 min. Samples were adjusted to 0.5% SDS. 10 μ g of EE antibody was added, and the samples were tumbled for 2 h at 4°C. Next, 20

μ l of Protein A/G PLUS agarose (Santa Cruz Biotechnology, Santa Cruz, CA) was added, and the sample was tumbled overnight at 4°C. The sample was centrifuged for 30 s at 200 × g to pellet the beads. The supernatant was discarded, and the beads were washed 3 times with 1 ml Extraction buffer. SDS-PAGE sample buffer containing 10 mM DTT was added to the washed beads, and the samples were heated at 65°C for 1 min (³H fatty acid labeled samples) or boiled for 5 min (³⁵S methionine/cysteine labeled samples). An aliquot was analyzed by 10% SDS-PAGE. Gels were incubated for 20 min in an aqueous solution of 50% methanol/10% acetic acid, followed by 10% ethanol/10% acetic acid for 20 min, and, finally, Amplify (Amersham) for 20 min. Gels were dried and subjected to fluorography at -80°C using Hyperfilm MP (Amersham). For ³⁵S pulse-chase experiments, intensity of each labeled band was quantitated by densitometry. Results were analyzed with GraphPad Prizm software to determine a half-life.

Acknowledgements

The author thanks Debra Garlin for technical assistance, Dr. Emiliana Borrelli for providing α_{i2} cDNA, Dr. Janine Morales for α_{i2} A327S cDNA, Dr. Henry Bourne for suggesting similarities with alternatively spliced H-ras, and Drs. Daniel Evanko and Jeff Benovic for critical reading of the manuscript.

Supported by National Institutes of Health Grant GM56444 and the Pew Scholars Program in the Biomedical Sciences.

References

1. Stow JL: **Regulation of vesicular transport by GTP-binding proteins.** *Current Opinion in Nephrology & Hypertension* 1995, **4**:421-5
2. Helms JB: **Role of heterotrimeric GTP binding proteins in vesicular protein transport: indications for both classical and alternative G protein cycles.** *FEBS Letters* 1995, **369**:84-8
3. Montmayeur J-P, Borrelli E: **Targeting of G α_{i2} to the Golgi by alternative spliced carboxyl-terminal region.** *Science* 1994, **263**:95-98
4. Picetti R, Borrelli E: **A region containing a proline-rich motif targets sG(i2) to the golgi apparatus.** *Experimental Cell Research* 2000, **255**:258-69
5. Marin EP, Krishna AG, Sakmar TP: **Rapid activation of transducin by mutations distant from the nucleotide-binding site: evidence for a mechanistic model of receptor-catalyzed nucleotide exchange by G proteins.** *J. Biol. Chem.* 2001, **276**:27400-5
6. Osawa S, Weiss ER: **The effect of carboxyl-terminal mutagenesis of Gt alpha on rhodopsin and guanine nucleotide binding.** *J. Biol. Chem.* 1995, **270**:31052-8
7. Thomas TC, Schmidt CJ, Neer EJ: **G-protein α_o subunit: Mutation of conserved cysteines identifies a subunit contact surface and alters GDP affinity.** *Proc. Natl. Acad. Sci. USA* 1993, **90**:10295-10299
8. Denker BM, Schmidt CJ, Neer EJ: **Promotion of the GTP-liganded state of the G α_{ox} protein by deletion of the C terminus.** *J. Biol. Chem.* 1992, **267**:9998-10002
9. Iiri T, Herzmark P, Nakamoto JM, van Dop C, Bourne HR: **Rapid GDP release from Gs alpha in patients with gain and loss of endocrine function.** *Nature* 1994, **371**:164-168
10. Posner BA, Mixon MB, Wall MA, Sprang SR, Gilman AG: **The A326S mutant of Gialpha as an approximation of the receptor-bound state.** *J. Biol. Chem.* 1998, **273**:21752-8
11. Pace AM, Faure M, Bourne HR: **Gi2-mediated activation of the MAP kinase cascade.** *Mol. Biol. Cell* 1995, **6**:1685-1695
12. Medina R, Grishina G, Meloni EG, Muth TR, Berlot CH: **Localization of the effector-specifying regions of Gi2alpha and Gqalpha.** *J. Biol. Chem.* 1996, **271**:24720-7
13. Wedegaertner PB, Chu DH, Wilson PT, Levis MJ, Bourne HR: **Palmitoylation is required for signaling functions and membrane attachment of Gq alpha and Gs alpha.** *J. Biol. Chem.* 1993, **268**:25001-8
14. Wedegaertner PB: **Lipid modifications and membrane targeting of G alpha.** *Biological Signals & Receptors* 1998, **7**:125-35
15. Resh MD: **Fatty acylation of proteins: new insights into membrane targeting of myristoylated and palmitoylated proteins.** *Biochim. Biophys. Acta* 1999, **1451**:1-16
16. Dunphy JT, Linder ME: **Signalling functions of protein palmitoylation.** *Biochim. Biophys. Acta* 1998, **1436**:245-61
17. Kopito RR: **Aggresomes, inclusion bodies and protein aggregation.** *Trends in Cell Biology* 2000, **10**:524-30
18. Johnston JA, Ward CL, Kopito RR: **Aggresomes: a cellular response to misfolded proteins.** *J. Cell Biol.* 1998, **143**:1883-98
19. Sunahara RK, Tesmer JJ, Gilman AG, Sprang SR: **Crystal structure of the adenylyl cyclase activator Gsalpha [see comments].** *Science* 1997, **278**:1943-7
20. Noel JP, Hamm HE, Sigler PB: **The 2.2 Å crystal structure of transducin α -GTP γ s.** *Nature* 1993, **366**:654-663
21. Coleman DE, Berghuis AM, Lee E, Linder ME, Gilman AG, Sprang SR: **Structures of active conformations of G α_i 1 and the mechanism of GTP hydrolysis.** *Science* 1994, **265**:1405-1412
22. Garcia PD, Onrust R, Bell SM, Sakmar TP, Bourne HR: **Transducin- α C-terminal mutations prevent activation by rhodopsin: a new assay using recombinant proteins expressed in cultured cells.** *EMBO J.* 1995, **14**:4460-4469
23. Grishina G, Berlot CH: **Identification of common and distinct residues involved in the interaction of alpha*i2* and alphas with adenylyl cyclase.** *J. Biol. Chem.* 1997, **272**:20619-26
24. Garcia-Mata R, Bebok Z, Sorscher EJ, Sztul ES: **Characterization and dynamics of aggresome formation by a cytosolic GFP-chimera.** *J. Cell Biol.* 1999, **146**:1239-54
25. Wang Y, Windh RT, Chen CA, Manning DR: **N-Myristoylation and betagamma play roles beyond anchorage in the palmitoylation of the G protein alpha(o) subunit.** *J. Biol. Chem.* 1999, **274**:37435-42
26. Fishburn CS, Herzmark P, Morales J, Bourne HR: **Gbetagamma and palmitate target newly synthesized Galphaz to the plasma membrane.** *J. Biol. Chem.* 1999, **274**:18793-800
27. Fishburn CS, Pollitt SK, Bourne HR: **Localization of a peripheral membrane protein: G beta gamma targets G alpha(z).** *Proc. Natl. Acad. Sci. USA* 2000, **97**:1085-1090
28. Evanko DS, Thiyagarajan MM, Wedegaertner PB: **Interaction with Gbetagamma is required for membrane targeting and palmitoylation of Galpha(s) and Galpha(q).** *J. Biol. Chem.* 2000, **275**:1327-36
29. Evanko DS, Thiyagarajan MM, Siderovski DP, Wedegaertner PB: **Gbeta gamma isoforms selectively rescue plasma membrane localization and palmitoylation of mutant Galphas and Galphaq.** *J. Biol. Chem.* 2001, **276**:23945-53
30. Lambright DG, Sondek J, Bohm A, Skiba NP, Hamm HE, Sigler PB: **The 2.0 Å crystal structure of a heterotrimeric G protein.** *Nature* 1996, **379**:311-319
31. Wall MA, Coleman DE, Lee E, Iniguez-Lluhi JA, Posner BA, Gilman AG, Sprang SR: **The structure of the G protein heterotrimer Gi $\alpha 1 \beta 1 \gamma 2$.** *Cell* 1995, **83**:1047-58
32. Hamm HE: **The many faces of G protein signaling.** *J. Biol. Chem.* 1998, **273**:669-72
33. Denker S, McCaffery JM, Palade GE, Insel PA, Farquhar MG: **Differential distribution of α subunits and $\beta\gamma$ subunits of heterotrimeric G proteins on Golgi membranes on the exocrine pancreas.** *J. Cell Biol.* 1996, **133**:1027-1040
34. Cohen JB, Broz SD, Levinson AD: **Expression of the H-ras proto-oncogene is controlled by alternative splicing.** *Cell* 1989, **58**:461-472
35. Faure M, Voyno-Yasenetskaya T, Bourne HR: **cAMP and $\beta\gamma$ subunits of heterotrimeric G proteins stimulate the mitogen-activated protein kinase pathway in COS-7 cells.** *J. Biol. Chem.* 1994, **269**:7851-7854
36. Wedegaertner PB: **Fatty acid acylation of G α .** In: *G Proteins: Techniques of Analysis* (Edited by: Manning DR) CRC Press, Boca Raton 1999, 153-171